Modeling Earth Systems and Environment
https://doi.org/10.1007/s40808-021-01321-2

ORIGINAL ARTICLE

Modeling the mixed layer depth in Southern Ocean using high resolution regional coupled ocean sea ice model

Anurag Kumar[1] · **R. Bhatla**[1,2]

Received: 26 August 2021 / Accepted: 15 October 2021

Abstract
The Southern Ocean (SO) is highly energetic and sensitive parts of the earth climate system. The regional scale upper ocean variability is highly dominant and energetic in SO. The interaction between the atmosphere and the ocean through mixed layer modulate the heat and nutrient exchange between the upper ocean surface and the dark deep ocean. Its space time variability modulates the distribution of carbon and water mass formation that influence the physical and biological pumps of SO. The mixed layer depth (MLD) generally calculated by climatological fields either by in-situ data or by numerical simulation. Here, we demonstrate the variability of mixed layer depth of SO in the domain 7° E–80° E; 72° S–45° S using a regional high resolution coupled ocean sea ice model. The model run is performed on a horizontal resolution at 9 km with open boundaries for a period of 20 years (1994–2013). The spatial and temporal variation of model-derived MLD is compared against the MLD of estimation the circulation and climate of the ocean 2 (ECCO2) reanalysis. The model has qualitatively as well as quantitatively good resemblance with ECCO2 reanalysis. The month-to-month MLD variation is very prominent, however, the model performance in simulation of seasonal MLD in open ocean is quite well compared to the higher latitude sea ice formation and melting domain. Along with this, an attempt has been made to understand and quantify the influence of air-sea forcing (near-surface zonal and meridional winds and air temperature) on the variability of mixed layer depth. The study shows the near-surface wind forcings have higher contribution to changing the MLD compare to atmospheric temperature, however, the effect of air temperature is also significant and prominent also in the study domain.

Keywords Southern Ocean · Mixed layer depth · Surface wind · Atmospheric temperature

Introduction

The mixed layer is a universal feature of the ocean where temperature, salinity, and density are vertically uniform. The vigorous oceanic turbulent processes take place in mixed layer depth (MLD) and mostly govern by the atmospheric fluxes (Cabrillo et al. 2011) such as, wind stress, heat, and fresh water exchange (Dwivedi et al. 2019). The transfer of mass, energy, and momentum from atmosphere to ocean through MLD is primary source of upper ocean motion and responsible for uniform density distribution (Villas Boas et al. 2019). Reversely, heat contained in MLD interacts directly with upper atmosphere and influence the atmospheric motion (Montegut et al. 2004). Therefore, the changes in MLD have a prime importance in changing the ocean–atmosphere mutual interaction (Yesubabu et al. 2020). The stable surface ocean leads to a shallower MLD due to less mixing while higher instability between the different layers of upper ocean is responsible for deep MLD (Somavilla et al. 2017). The behavior and depth of mixed layer is depends on the advection, diffusion, and turbulent physical processes. The transfer of heat and momentum through buoyancy and wind by air–sea interaction also modulate the MLD (Bharti et al. 2019) and the change in MLD can directly influence the predictability of ocean sea surface temperature, ocean biogeochemical distribution etc. (Alexander and Deser 1995; Dommenget and Latif 2002; Deser et al. 2003; Fransner et al. 2020). For example, the study of Bessa et al. 2020 reported the deeper/shallower MLD respond to minimum/maximum sea surface temperature. Apart from this the MLD has its own importance in the

✉ R. Bhatla
rbhatla@bhu.ac.in

[1] Department of Geophysics, Institute of Science, Banaras Hindu University, Varanasi, India

[2] DST-Mahamana Centre of Excellence in Climate Change Research, Banaras Hindu University, Varanasi 221005, India

Published online: 29 October 2021

field of acoustic propagation (Sutton et al. 1993), biology (Fasham 1995), and in understanding air–sea interactions involving air-sea heat budget, buoyancy, and momentum exchange (Chen et al. 1994). The MLD controls the nutrient availability as well as phytoplankton exposure to light and thus its great relevance for phytoplankton growth (Mitchell and Holm-Hansen 1991; Biggs et al. 2019). To understand the above physical processes well the correct estimation of MLD is highly need. Also the ocean surface layer exhibit large temporal and spatial variability than rest of the ocean so it in important to understand the MLD variability and its relation with air–sea interaction on short-term and long-term scale (Bessa et al 2018). On the regional scale the different atmospheric fluxes have different effects in the modulation of MLD (Pookkandy et al. 2016), so it is important to decipher the role of different atmospheric fluxes on the variability of MLD on different sector of SO (Fischer 2000; Kara et al. 2003; McCreary et al. 2001; Zhang and Marotzke 1999). Therefore, in the present study, the MLD variability in SO around (7° E–80° E; 72° S–45° S) and the effect of atmospheric forcing on the MLD variation is studied. Deep mixed layers in SO are linked to Antarctic Intermediate Water (AAIW) and Subantarctic Mode Water (SAMW) formation (Hanawa and Talley 2001). Also, the upper and lower limbs of global overturning circulation, which carries heat throughout the globe has precisely linked with the processes of AAIW and SAMW formation (Sloyan and Rintoul 2001). In the vicinity of Antarctica Circumpolar Current summer MLD reaches about 100 m in the Southern Ocean region, however, in the winter time due to cooling the water column destabilizes and increases the MLD. A recent study (Dong et al. 2007) on MLD in Southern Ocean suggests that to obtain a realistic ocean thermal balance involving air–sea interaction a proper representation of the temporal variations of MLD is very important. Most of the anthropogenic carbon stored by the Southern-Hemisphere oceans have accumulated in the intermediate waters whose properties are set in the mixed layer of the Southern Ocean (Sabine et al. 2004). The contribution of the SO in the global carbon cycle (Frolicher et al. 2015; Marshall and Speer 2012), the uptake of anthropogenic carbon that enters into the ocean (Gruber et al. 2009; Khatiwala et al. 2009) and upwelling of nutrient rich water (nearly 80%) (Lumpkin and Speer 2007; Talley 2013) makes SO very important for modulation of MLD. Also reversely, the cycling of carbon in SO strongly depends on ML (Sabine et al. 2004; Sallée et al. 2012; Verdy et al. 2007). Along with this, the regional scale MLD of SO is also connected with mid-latitudes and tropical phenomena (Kidston et al. 2011; Bader et al. 2013; Yuan and Martinson 2000; Martinson and Iannuzzi 2003; Yuan 2004). Therefore, for better understanding about these processes, the correct estimation of the SO mixed layer depth variability in SO is highly need.

The presence of sea ice at high latitude makes this region more complex to study about atmosphere–ocean interaction due to mutual interaction between atmosphere, ocean, and sea ice. The SO sea-ice directly influence our marine ecosystem and climate by water mass transformation (by changing MLD) and sea ice–ocean interaction. The presence of sea ice in polar areas has a strong effect on MLD at high latitude. The study done by Petty et al. (2014) shows the net salt flux from sea ice growth/melt dominates the evolution of the mixed layer over the Antarctic shelf seas. Sea ice takes heat and momentum (energy balance) directly from the air while it generates buoyancy fluxes at the sea surface when it forms or melts. This sea ice energy balance is also getting affected by the modulation of heat flux of MLD at the base of ice layer (Pellichero et al. 2017). The formation and melting of sea ice together with the mixing of surface layer currently poorly represented in large-scale ocean-sea ice models. Apart from this the presence of sea ice in SO, its formation and decomposition has a direct effect on the modulation of MLD in different parts of the SO that can affect the regional scale air–sea interaction and oceanic properties. Therefore, it is important to study about SO MLD variability with inclusion of sea ice physics on a regional scale to incorporate the ice–ocean interaction together.

However, due to lack of long-term observations in the Southern Ocean and coarser resolution model output, the SO MLD variability and its response to atmospheric forcing has not been studied very well (Cabrillo et al. 2011). The time varying observation data are very limited and few for high latitude SO for obvious regions (complex environment). Moreover, compared to the other sectors (Atlantic and Pacific) of SO, the MLD along Indian Ocean sector of SO has remained largely unexplored. This, therefore, limits our understanding about the MLD variability and its response with atmospheric fluxes around this sector. Apart from this the two Indian Antarctic stations Maitri and Bharati are located in the chosen study domain. The correct representation of MLD variability in the study region can provide a better understanding about ocean stability (mixing) which can help in ship navigation by different scientific organization time to time to collect the data around both Indian Antarctic stations for research purpose. Therefor to fill this gap and to understand the variability of MLD in SO around [7° E–80° E; 72° S–45° S] we run a limited area, high resolution coupled ocean sea ice model at 9 km horizontal resolution with various sensitivity experiments to see the role of atmospheric forcing on MLD variability. In general MLD have been mostly defined in two ways first one based on specifying a difference in temperature or density from the surface value (Wyrtki 1964; Levitus 1982) and the other one is based on specifying a gradient in temperature or density (Bathen 1972; Lukas and Lindstrom 1991). Here we are using a new criterion, (Lorbacher et al. 2006) based

on the shallowest extreme curvature of near-surface layer density or temperature profiles to calculate MLD.

The present paper attempts to understand the monthly and seasonal mean variability of the mixed layer in the aforesaid domain by use of state of the art high resolution coupled ocean sea ice model. As the MLD is stronger depends on air-sea fluxes so the second aim of this manuscript is to understand the role of wind and atmospheric temperature on MLD variability. This paper is organized as follows. Section 2 gives a brief detail about data and methods. The results and discussion are given in Sect. 3. Conclusions are in Sect. 4.

Data and methods

Model description

The high resolution coupled ocean sea ice Massachusetts Institute of general circulation model (MITgcm) (Marshall et al. 1997) is implemented in a limited area of SO (7° E–80° E; 72° S–45° S). The MITgcm is a Z-coordinate model and solves the incompressible Navier–Stokes equations. The different categorization of sea ice thickness in MITgcm is scholarly important to use it at high latitude (Campin et al. 2008). The hydrostatic approximation is used in our model simulation. The physical configuration is based on Arakawa C-grid with a horizontal resolution of 9 km. The 28 vertical level discretization retained in the model simulation with highest vertical resolution of 5 m on surface decreasing to 700 m at the bottom and 13 vertical levels within the depth of 120 m. The corresponding vertical depths used in the model simulation are shown in Table 1. To discretize the vertical mixing in the model simulation the K profile parameter (KPP) scheme (Large et al. 1994) is used. The bathymetry used in model domain is derived from the smith and sandwell 1' data (Smith and Sandwell 1997) and shown in Fig. 1. To get a stable model solution, the diffusion coefficient of temperature and salinity are taken as 10^{-5} m^2/s and the bottom frictional drag coefficient is 0.001. The Jacket and McDougall (1995) nonlinear equation of state is used in the model simulation. To force the model 10-m atmospheric winds, 2-m air temperature, radiation (long wave and short wave), humidity, runoff, and precipitation (a sum of liquid and solid) on daily frequency are used. The model uses the bulk formula of Large and Pond (1982) to convert these atmospheric forces into corresponding fluxes. The atmosphere–ocean mutual interaction drives the ocean circulation and MLD at high latitude in SO and can be moderated by sea ice formation and melting. Therefore, for proper representation of the ocean and MLD variability at high latitude a well-coupled ocean sea-ice model is required by realistic physics. Hence, for an accurate representation of MLD, we used build in dynamical and thermo-dynamical sea ice package of MITgcm. The dynamical package of sea ice is

Table 1 Central depth of the vertical levels of the ocean sea ice model

Level	Central depth (m)
1	2.5
2	7.5
3	12.5
4	17.5
5	22.5
6	27.5
7	33.0
8	40.0
9	49.0
10	60.5
11	75.5
12	95.0
13	120.0
14	151.5
15	191.5
16	241.5
17	304.0
18	384.0
19	489.0
20	624.0
21	799.0
22	1024.0
23	1324.0
24	1724.0
25	2199.0
26	2749.0
27	3399.0
28	4099.0

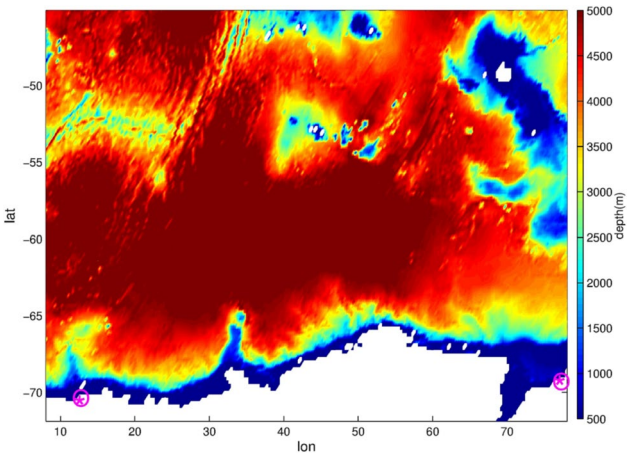

Fig. 1 Bathymetry of the model domain in the Southern Ocean [7° E–80° E; 72° S–45° S]. Matri and Bharati Indian Antarctic stations are marked by circle

based on elastic–viscous–plastic (EVP) rheology (Hunke and Dukowicz 1997) which is written on Arakawa C-grid. The Line successive over-relaxation (LSOR) solver is implemented to solve the sea ice equations. To incorporate the thermo-dynamical contribution of sea ice in the model solution, we used the three-layer sea ice model of Winton (2000). The albedo values are chosen by different efforts of model simulation and taken as 0.19, 0.80, 0.68, 0.89, and 0.90 for open water, dry ice, wet ice, dry snow, and wet snow, respectively. We derived the model output on a daily frequency for a period of 24 years (1990–2013). The model reaches a stable solution within the initial 4 years (1990–1993) and data from 1994 to 2013 (20 years) are taken for analysis. In an effort to demonstrate the effect of air-sea forcing variables on the variability of MLD, we performed three different sensitives (inter-compression) experiments. In the first experiment hereinafter referred to as CTRL run, we force the model with daily data of winds, air temperature, relative humidity, downward short-wave, and long-wave radiation and precipitation. In the second experiment hereinafter known as WWIND, we do not use the zonal and meridional wind to force the model and all other forcings are as same as CTRL experiment. Similarly, in the third and last experiment, hereinafter referred to as WATEMP we do not use atmospheric temperature (there is no air-atmosphere fluxes) to force the model while keeping all the forcing as similar to CTRL run.

Data

The initial conditions of temperature and salinity to initialized the model are taken from the World Ocean Atlas 13 (WOA13) (Johnson et al. 2013) at 25 km resolution and sea ice concentration from GIOMAS at 100 km resolution. These data are then interpolated on our model grid at 9 km. To force the model the atmospheric fields, 10-m atmospheric winds, 2-m air temperature, radiation (long wave and short wave), relative humidity, runoff, and precipitation are taken from The National Centers for Environmental Prediction (NCEP) and the National Center for Atmospheric Research (NCAR) (Kalnay et al. 1996). To incorporate the ocean boundary conditions the temperature, salinity, zonal, and meridional current are taken from the estimating the circulation and climate of the ocean 2 (ECCO2) (Menemenlis et al. 2008) reanalysis, and prescribed at each boundary. The model computes the net flow across the boundaries and adjusts all normal velocities on boundaries to obtain zero net flow. The boundaries values are updated on the time interval of 30 days. The boundary conditions for sea ice (sea ice concentration, sea ice thickness and snow thickness) are taken from global ice-ocean modeling and assimilation system (GIOMAS) (Zhang and Rothrock 2003). The model output ocean temperature, ocean salinity, zonal, and meridional velocity at each depth are stored on daily basis for analysis.

Results and discussion

The coupled ocean sea ice model MITgcm is configured on a regional scale 7° E–80° E; 72° S–45° S in SO domain. The details of the model configuration are given in Sect. 2. We performed three experiments, CTRL, WWIND, and WATEMP as described above for a period of 20 years [1994–2013]. Before discussing the sensitivity experiments, it would be useful to discuss the ability of the model to capture the MLD variability in the study domain. For this purpose, estimating the circulation and climate of the ocean 2 (ECCO2) reanalysis MLD is used for model validation. The monthly climatological MLD values (annually averaged) of ECCO2 and model is shown in Figs. 2 and 3, respectively. The high and low MLD variability is clearly captured by the model with maximum in winter months (July, August, and September) and lower in summer months (January, February and March). The shallow MLD (< 50 m) during summer months is because of the freshness of the ocean water due to sea ice melting. However, it is noted that the model is performing better to represent MLD variability above 55° S (open ocean; 7° E–80° E, 55° S–45° S) than below 60° S (region of sea ice formation and melting; 7° E–80° E, 70° S–60° S) for each month. The discrepancy of MLD values in the sea ice melting/formation domain may be because of the coarse resolution (25 km) of ECCO2 reanalysis data. Another possible cause could be the uncertainties in air-sea forcing at high latitude. The highest MLD (more than

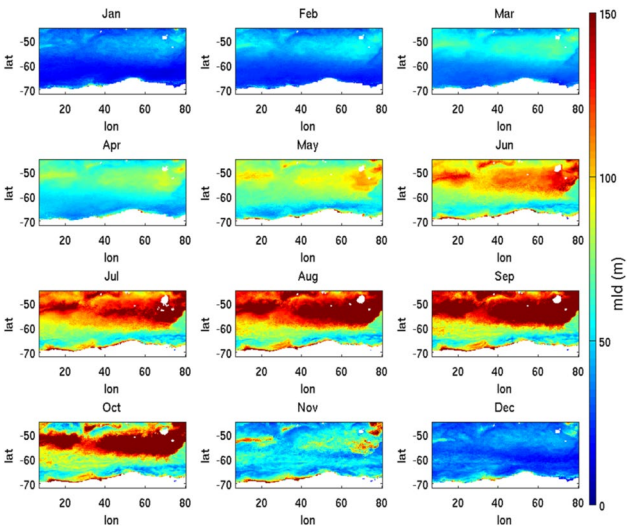

Fig. 2 ECCO2 derived monthly variability of mixed layer depth (in meter) of the region for each months of the year. The values are climatological mean over the period 1994–2013

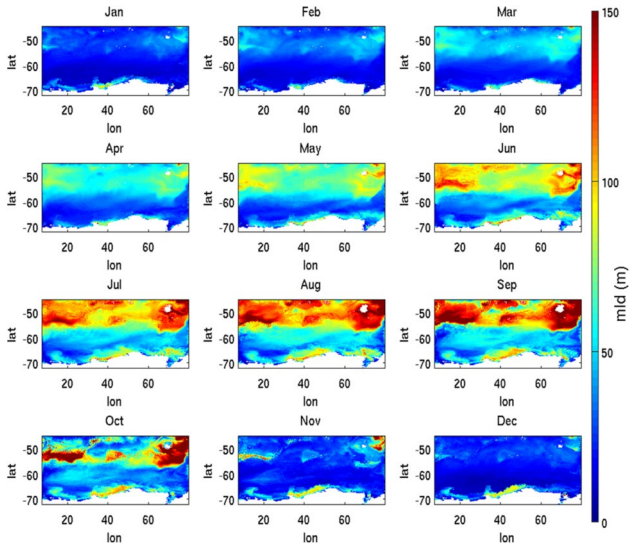

Fig. 3 Model derived monthly variability of mixed layer depth (in meter) of the region for each months of the year. The values are climatological mean over the period 1994–2013

100 m) is found in winter months (June, July, August, and September) open ocean. It is also noted that along the south boundary the model-derived MLD are consistent with ECCO2 in summer months while for winter months (June, July, August, and September) model MLD is overestimating along the land–ocean interface. The above results depict different MLD variability in the study domain. The high MLD values in open ocean for winter is due to more stable and intense wind of SO in winter time than summer. The lower value of MLD below 60° S is due to formation and melting of sea ice. For example, in winter (June, July, August, and September) the formation of sea ice at high latitude prevent the transfer of momentum and heat flux into the ocean through the atmosphere, hence the mixing and diffusion can reduce on the upper surface that can reduce the MLD at higher latitude compare to open ocean. Similarly, in summer months, the higher sea surface temperature gives more melting of sea ice at high latitude and hence more freshness which leads the less MLD value. It is clear from Figs. 2 and 3 that MLD values are minimum for the month of January then start to increases, becomes maximum in the month of September and onwards then it starts to decrease. The huge transition of MLD values from the month of October to November is seen and this feature is clearly captured by the model. The above discussion shows the prominent MLD variation even in a small study domain and our regional coupled ocean sea-ice model is reasonably able to capture this variability. Some inconsistency with the model MLD solution against ECCO2 reanalysis may be due to the uncertainty in model parameterization and forcing. We will try to reduce the existing biases of MLD in the next part of our study with help of data assimilation and using more high-resolution atmospheric forcing.

To further examine the variability of MLD and to put the results into perspective we have plotted the seasonal map of model-derived MLD with ECCO2 MLD in Fig. 4. The season chosen for this purpose are Jan–Feb–Mar, Apr–May–June, Jul–Aug–Sep, and Oct–Nov–Dec. The model MLD values are close to the ECCO2 MLD estimates in all the seasons, however, model-derived MLD is quite well in the open ocean compared to the domain of sea ice formation and melting. Moreover, we notice deeper MLD in the open ocean compare to high latitude while the MLD remains low along the coastal parts of the southern boundary. The lowest MLD values are observed in the season of Jan–Feb–Mar and highest during Jul–Aug–Sep. The mean MLD in the open ocean domain during Jan–Feb–Mar, Apr–May–Jun, Jul–Aug–Sep, and Oct–Nov–Dec are 30, 90, 130, and 75 m, respectively. On the other hand, mean MLD for these seasons are 10, 45, 65, and 40 m, respectively, in sea ice melting and formation domain. Thus, the mean MLD of the open ocean remains high compare to mean MLD of

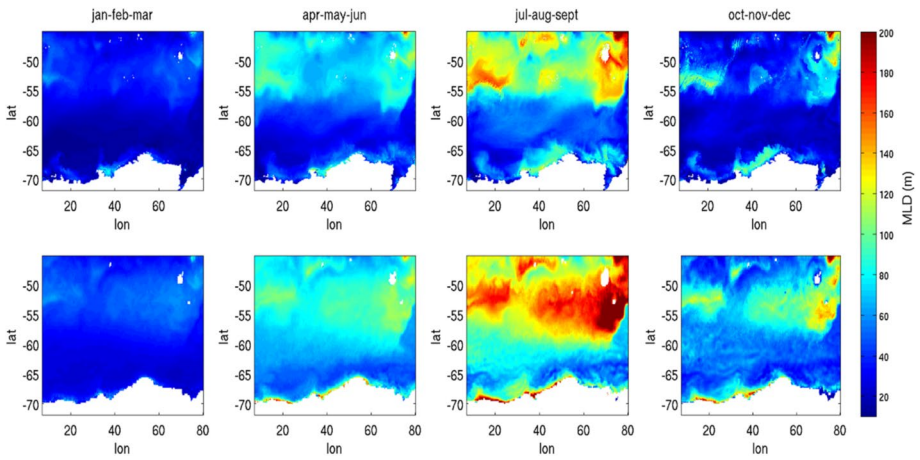

Fig. 4 Seasonal variability of mixed layer depth (in meter) of the region during the season Jan–Feb–Mar, Apr–May–Jun, Jul–Aug–Sep, and Oct–Nov–Dec over the period 1994–2013. The ECCO2 and model-derived MLD is shown in 1st and 2nd row, respectively

sea ice formation and melting region. It is notice that during Jul–Aug–Sep the open ocean region shows high MLD values whereas the southern part of the domain (sea ice formation and melting region) shows comparatively low MLD. The lower MLD in the study domain during the summer season may be because of complete sea ice melting that provides more freshwater to the ocean and hence less stratification and low MLD. Similarly, in the winter season the cold and intense wind of SO enhances the strength of the Antarctic circumpolar current that can produce deep mixing and hence high MLD. Figure 4 shows that the season to season MLD variability is quite significant and this feature is clearly demonstrated by the model well.

In the line of evaluation of model performance in MLD simulation, we have plotted area-averaged monthly time series of model-derived and ECCO2 MLD in the two distinct domains ([sea ice formation and melting, 7° E–80° E, 71.8° S–60° S] and open ocean, [7° E–80° E, 55° S–45° S]) in 1st and 2nd row of Fig. 5, respectively. For the 1st row of Fig. 5 it is seen that the model MLD have the same temporal variability as ECCO2 MLD in the sea ice melting and formation domain [7° E–80° E; 71.8° S–60° S] with a correlation coefficient of 0.82 (99.9% significant), however, the model MLD is underestimated in the range of 10 m in winter months of each year. It is also noted that the maximum value of MLD is found in the winter months and minimum in summer months. It is interesting to note, MLD in the winter months is sharply declines for the year 2008 and becomes minimum compare to other years, and this feature is clearly captured by the model. Similarly, from 2nd row of Fig. 5 we found that MLD is nearly periodic in the open ocean domain with the maximum in winter and minimum in summer. The model is clearly able to capture the MLD variability in this domain with a correlation coefficient of 0.93 (99% significant). The largest mis-discrepancies are seen for the year 2003–2006. It is noted that model-derived MLD in the region [7° E–80° E, 55° S–45° S] is nearly twice in the magnitude compare to MLD of the region [7° E–80° E; 71.8° S–60° S]. Further, we found the standard deviation of MLD time series of model and ECCO2 is 18.2 and 22.7 and 36.9 and 45.0 in the domain [7° E–80° E; 71.8° S–60° S] and [7° E–80° E, 55° S–45° S], respectively. The overall performance of model MLD in these two different domains in terms of temporal variation, correlation coefficient and standard deviation shows that model has a good resemblance with ECCO2 in simulation of MLD. The above results clearly showing that our coupled ocean sea-ice model is able to capture the MLD variability on monthly, seasonal and temporal scale for the aforesaid time period. We have investigated the area-averaged (over the all study domain [7° E–80° E; 71.8° S–45° S]) monthly MLD time series of model and ECCO2 in Fig. 6. The correlation coefficient between the model and ECCO2 derived MLD is 0.9450 which shows the robustness of model performance to derive the MLD solution in the entire study domain. The shallow MLD (20–35 m) is found in summer months (Jan–Feb–Mar) whereas the deep MLD (65 m–75 m) during winter months (Jan–Feb–Mar).

The exchange of momentum, heat, and radiation from atmosphere to ocean through air-sea forcing has a prominent

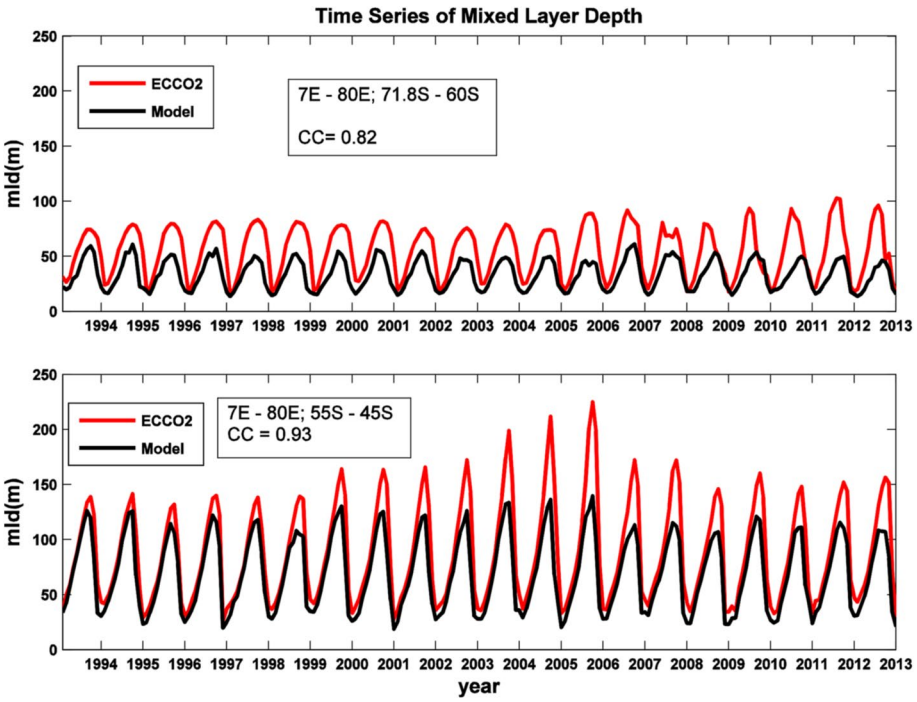

Fig. 5 Monthly time series of mixed layer depth (in meter) area averaged over the region (1st row) [7° E–80° E; 60° S–71.8° S] and [7° E–80° E; 55° S–45° S] (2nd row). The red line represents the ECCO2 derived MLD whereas the black line is showing the model simulated MLD

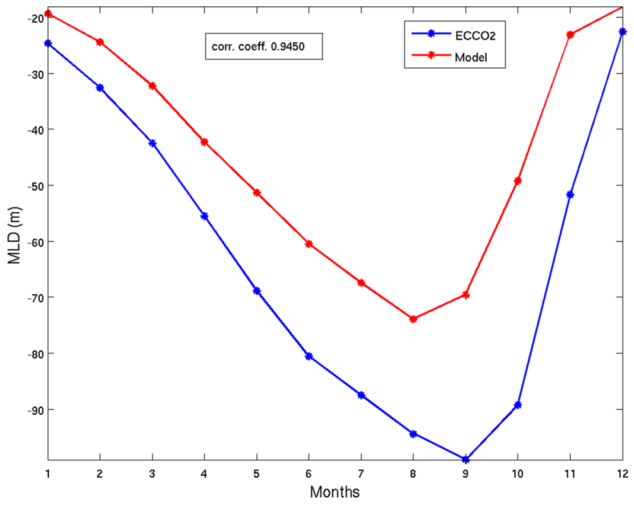

Fig. 6 Monthly climatological time series of mixed layer depth (in meter) area averaged over the region [7° E–80° E; 45° S–71.8° S]. The blue line represent the ECCO2 derived MLD whereas the red line is showing the model simulated MLD

influence on the variability of MLD. To further investigate the role of the atmosphere in the modulation of MLD in the study domain, we have performed the two sensitive experiments WWINDS and WATEMP as described in Sect. 2. Figure 7 represents monthly MLD variation for WWINDS experiment in which wind is not used to force the model. It is clear from Fig. 7 that MLD is decreasing fast in the absence of wind in all months. It is because, in the absence of wind the mixing along the upper ocean remains low which leads to shallow MLD. The highest decrease is seen in the months of January and February where MLD remains low (5–10 m). The MLD in the absence of wind is also decreasing for the months of July and August as compared to CTRL run, however, it remains high compare to other months in the absence of wind. Further, it is seen that MLD remains high along the southern boundary in the absence of winds. It is found that for WWINDS experiment a water mass of high MLD values (70–90 m) along the north-east domain is starting to generate from the month of May and becomes maximum in September and then starts to decrease from October then disappear in the month of December. In the absence of wind, no direct interaction of the atmosphere with the upper surface of the ocean, therefore, momentum is not transfer properly, thus weak vertical mixing and wind stress curl which cannot properly mix heat flux and energy and hence weak and shallow mixed layer. The physical mechanism for the transfer of heat and momentum through the atmosphere–ocean in the absence of wind is further explained by the model used mathematical formula in the section appendix of this draft.

To further see the effect of wind on monthly MLD variability we have plotted the difference of model-derived MLD of WWINDS from CTRL run MLD in Fig. 8. The MLD differences (CTRL-WWINDS) become highly positive in the open ocean domain (55° S–45° S) as compared to the high latitude (68° S–60° S) in all the months except for the months of November and December. Thus in the absence of near-surface wind MLD of the open ocean region is highly decreases due to lack of momentum transfer, vertical mixing and associated physical processes. The highest difference in MLD (> 50 m) is seen in open ocean from April and becomes maximum in September. From October these differences start to decrease and minimum in December. This shows, wind is playing a major role in the modulation of the MLD in open ocean even on the monthly time scale. Further, we have seen that the MLD of the open ocean in the absence of wind for winter months (Jun–Jul–Aug) is greatly

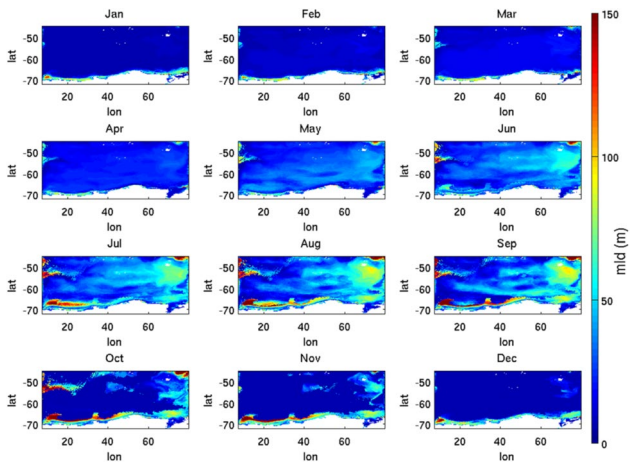

Fig. 7 Model derived monthly variability of mixed layer depth (in meter) of the region for each months of the year for WWINDS experiment. The values are climatological mean over the period 1994–2013

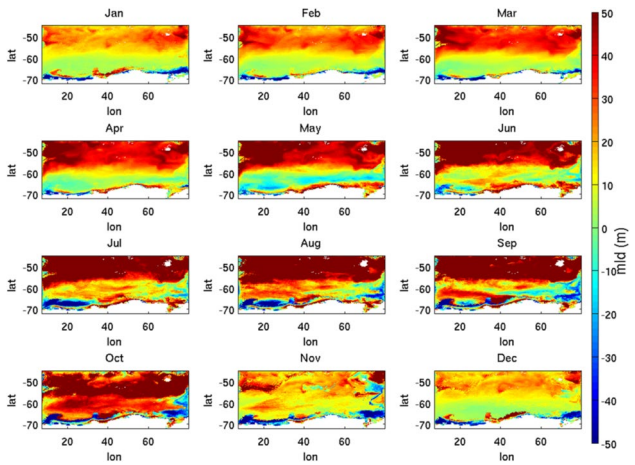

Fig. 8 Maps of monthly MLD differences between CTRL and WWINDS experiments. The values are climatological mean over the period 1994–2013

decreasing. It may be because, in these months nearly all domain shall be fully covered by the sea ice which decreases upper water stratification that leads to lower MLD. For the high latitude domain (68° S–60° S) the MLD differences are less as compared to the open ocean. For the month of January, February, March, and April the MLD differences in this region are in the range of 10–15 m. It is interesting to note that for the month of May the MLD differences become negative. Onwards from June the differences in MLD again start to become positive and approaches a maximum (> 35 m) in the month of October and then again start to decrease for next months. The above discussion shows the wind is playing a major role in changing the MLD around the high latitude domain also. It is also noted that the MLD differences along the southern boundary remain negative in each month. It may be because the presence of sea ice in the southern coastal domain during all months can eject the brine pockets in higher quantity that can create higher density gradient at the ocean surface in the absence of near-surface wind forcing (no proper mixing), these denser water moves downward thus result into increase in MLD.

In the line of investigation about the role of air-sea in changing the MLD, we have performed another experiment WATEMP (no air-temperature is used to force the model). Figure 9 represents the monthly MLD variation for WATEMP experiment. The nature of monthly MLD variability for WATEMP experiment is nearly the same as the monthly MLD of CTRL run but the magnitude is changing (increase/decrease) in different parts of the study domain. The maximum MLD in the open ocean domain is seen for the months of June, July, and August and MLD reaches up to 150 m. The MLD values are then start to decrease fast from October and retain the lowest in the months of January. It is interesting to note that for the higher latitude domain [68° S–60° S; 7° E–80° E], the MLD is changing very little approximately in the range from 5 to 10 m as compared to CTRL run. It is noted that for the months of January to June the MLD at higher latitude changes significantly and the nearly the same MLD value as the actual model solution (CTRL), however, the MLD of WATEMP experiment in this region is decreasing for the months of June–October. It is also noted that the MLD along the central southern boundary is changing (increasing) compare to CTRL run for the month of May to October. The analysis shows the month-to-month variation in MLD of WATEMP experiment is quite significant with different magnitudes in different parts of the study domain.

To see the dependency of MLD variability on air temperature, we have plotted the difference between CTRL run MLD with MLD derived in WATEMP experiment in Fig. 10. It is seen that difference is either zero or very less positive in the entire study domain for the month of January, February, and March. However, negative differences are present along the northern boundary interface in these months. It is further found that in the open ocean domain the positive differences start to decrease onwards from January and then become more negative in June and highest negative in September. However, along the southern boundary, the highest positive differences (more than 30 m) are seen for the month of January which starts to decrease and becomes negative at some places. In the month of June, these negative differences along the southern boundary are highest (> − 30 m) with some very less positive differences at few places. For the high latitude (sea ice formation and melting domain), the differences in MLD are positive in all months and maximum (> 40 m) in the month of October and then start to decrease in magnitude from November. The low MLD values (shallow

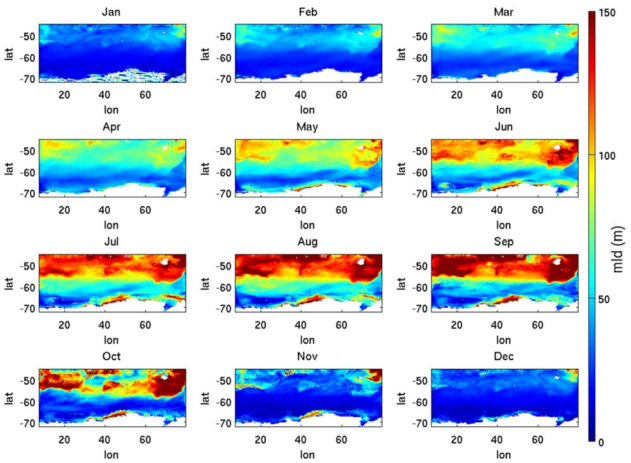

Fig. 9 Model derived monthly variability of mixed layer depth (in meter) of the region for each months of the year for WATEMP experiment. The values are climatological mean over the period 1994–2013

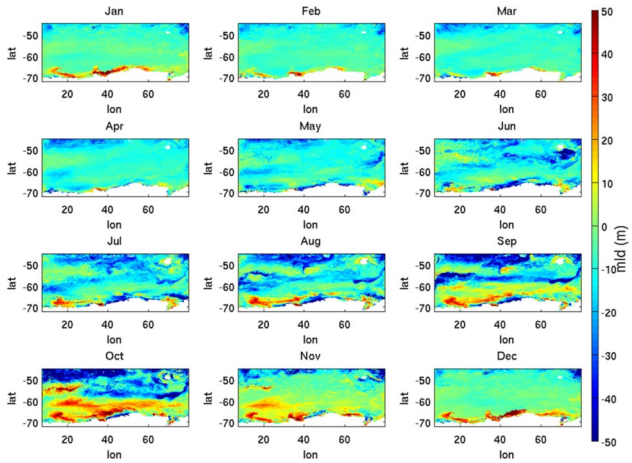

Fig. 10 Maps of monthly MLD differences between CTRL and WATEMP experiments. The values are climatological mean over the period 1994–2013

MLD) in peak winter months (Jun–Jul–Aug–Sep) for WATEMP experiments occurs since in the absence of air temperature, the SST becomes low that leads to less stratification results in shallow MLD. This analysis shows that atmospheric temperature have also a prominent role in changing the MLD of the region. The overall results are showing the air-sea forcing has a great role in the modulation of MLD of the domain on monthly to seasonal scale. It is also demonstrated that the wind has a major role in influencing the MLD compare to atmospheric temperature.

Conclusions

The ocean mixed layer is worldwide important for the world oceanography. The depth of mixed layer influences directly the exchange of heat, carbon, moisture, and gases between ocean and atmosphere by air–sea interaction and becomes one of major factor to control the ocean productivity. In this study, we configure and run a limited area, high resolution (9 km) regional coupled ocean sea ice model to investigate the variability of mixed layer depth (MLD) in the region [7° E–80° E; 72° S–45° S] of the Southern Ocean (SO). The spatial and temporal variability of model-derived MLD is compared against the MLD of ECCO2 reanalysis. It is found that the model is reasonably able to represent MLD variability well in the study domain on monthly to seasonal scale. The model-derived MLD temporal variability is nearly periodic in the nature and coherent with ECCO2 MLD. The month-to-month variability of MLD is very prominent during the simulation period with maximum MLD in winter months compared to the summer months. It is found that the model performance to decipher the variability of MLD is quite better in open ocean compare to sea ice formation and melting region. Our coupled ocean sea ice model simulation also conclude that the formation and melting of sea ice directly modulate MLD in terms of stratification. The ejection of more brine along the southern boundary is responsible for high MLD due to formation of heavy water masses. The effect of air-sea forcings on monthly MLD variability is also investigated by performing two sensitivity experiments WWINDS and WATEMP by our regional configuration of MITgcm. In the absence of wind the highest decrease is found for the months of January and February. It is concluded that for the winter months the model MLD in the absence of wind is decreasing as compared to CTRL run. Further it is concluded, the nature wise the MLD variability for WATEMP experiment of model is same as CTRL run but the magnitude is changing with maximum MLD in winter months. For the entire study period it is found that near-surface winds have a major contribution in the modulation of MLD in the study domain compare to atmospheric temperature.

Appendix

The wind stress and the surface heat fluxes are calculated by following bulk formulas of the model from the air-sea forcing fields:

Wind stress

The corresponding wind stress from the zonal and meridional wind is computed by model as below:

$$\tau_{\mu} = c_d * \rho_a * W_s * u_{10}, \tag{1}$$

$$\tau_{v} = c_d * \rho_a * W_s * v_{10}, \tag{2}$$

where ρ_a is surface density of the air and calculated by from atmospheric forcing fields, c_d is the drag coefficient u_{10} *and* v_{10} are the 10-m zonal and meridional winds. The drag coefficient for wind speed 4–11 m/s is taken as 1.2×10^{-3} and $(0.49+0.065\,W_s)\times10^{-3}$ for wind speed 11–35 m/s.

Surface heat flux

The below are the computational formulas which model uses to compute surface heat flux from provided air-sea forcing:

$$Q_{\mathrm{hflux}} = -Q_{\mathrm{hs}} - Q_{\mathrm{hl}} + Q_{\mathrm{lwf}} + Q_{\mathrm{swf}}, \tag{3}$$

where Q_{hs} and Q_{hl} are the sensible and latent heat flux in to the ocean, respectively. Q_{lwf} and Q_{swf} are net long-wave and net short-wave radiation flux to the atmosphere, respectively.

The sensible heat flux Qhs and the latent heat flux are calculated in the model as:

$$Q_{\mathrm{hs}} = c_h * \rho_a * C_{\mathrm{pa}} * W_s * \mathrm{del}\,T, \tag{4}$$

$$\mathrm{Qhl} = \rho_a * c_e * L_{\mathrm{vap}} * W_s * \mathrm{del}Q, \tag{5}$$

where ρ_a the density of air at surface, c_e $(0.0346\times\sqrt{c_d})$ is the Dalton number and ch $(0.0327\times\sqrt{c_d})$ is the Stanton number. C_{pa} is the specific heat of air at constant pressure (1005 J kg^{-1} K^{-1}), L_{vap} is the latent heat of vaporization (2.5×10^{6} J kg^{-1}), del$T$ and del Q is the difference of temperature (air) and difference of specific humidity at 2 m and surface. The net long-wave radiation and net short-wave radiation flux is given by:

$$Q_{\mathrm{lwf}} = \varepsilon\sigma T^4 - Q_{\mathrm{dlw}}, \tag{6}$$

$$Q_{swf} = Q_{dsw}\,(1 - \alpha), \tag{7}$$

where ϵ is the ocean emissivity (0.98), σ is the Boltzmann constant, T is surface temperature and Q_{dsw} is the downward long-wave radiation and $\alpha$is albedo.

WWINDS and WATEMP experiment

In the absence of 10 m wind, the wind stress will be zero from Eqs. (1) and (2). Also the sensible and latent heat flux will also be zero from Eqs. (4) and (5) and the surface heat flux which now contributes in MLD variation will be only from downward short- and long-wave radiation.

Similarly, in the absence of air temperature the energy exchange between ocean and atmosphere will be change [(1–7)] which can influence the planetary boundary layer of the atmosphere. The cooling in the atmosphere in the absence of air temperature will reduce the turbulent transport and also the role of surface heat fluxes which can lead to modulation in MLD.

Acknowledgements AK is thankful to Department of Science and Technology, Government of India for providing Science and Engineering Research Boar National Post-Doctoral Fellowship (SERB NPDF) with file number PDF/2019/001585 under which this work is carried out. Authors are also thankful to the ECCO2, NCEP/NCAR, WOA13 and GIOMAS communities to provide their data freely.

References

Alexander MA, Deser C (1995) A mechanism for the recurrence of wintertime mid-latitude SST anomalies. J Phys Ocean 25:122–137

Bader J, Flugge M, Kvamsto NG, Mesquita MD, Voigt A (2013) Atmospheric winter response to a projected future Antarctic sea-ice reduction: a dynamical analysis. Clim Dyn 40:2707–2718

Bathen KH (1972) On the seasonal changes in the depth of mixed layer in the north Pacific Ocean. J Geophy Res 77:7138–7150

Bessa I, Makaoui A, Hilmi K, Afifi M (2018) Variability of the mixed layer depth and the ocean surface properties in the Cape Ghir region, Morocco for the period 2002–2014. Model Earth Syst Environ 4(1):151–160

Bessa I, Makaoui A, Agouzouk A, Idrissi M, Hilmi K, Afifi M (2020) Variability of the ocean mixed layer depth and the upwelling activity in the Cape Bojador, Morocco. Model Earth Syst Environ 6(3):1345–1355

Bharti V, Fairall CW, Blomquist BW, Huang Y, Protat A, Sullivan PP, Siems ST, Manton MJ (2019) Air-sea heat and momentum fluxes in the Southern Ocean. J Geophys Res-Atmoss 124:12426–12443

Biggs TE, Alvarez-Fernandez S, Evans C, Mojica KD, Rozema PD, Venables HJ, Pond DW, Brussaard CP (2019) Antarctic phytoplankton community composition and size structure: importance of ice type and temperature as regulatory factors. Pol Biol 42:1997–2015

Cabrillo RS, González-Pola C, Ruiz-Villarreal M, Montero AL (2011) Mixed layer depth (MLD) variability in the southern Bay of Biscay. Deepening of winter MLDs concurrent with generalized upper water warming trends? Ocean Dyn 61(9):1215–1235

Campin JM, Marshall J, Ferreira D (2008) Sea ice-ocean coupling using a rescaled vertical coordinate z. Ocean Model 24:1–4

Chen D, Busalacchi AJ, Rothstein LM (1994) The roles of vertical mixing, solar radiation, and wind stress in a model simulation of the sea surface temperature seasonal cycle in the tropical Pacific Ocean. J Geophys Res 99:20345–20359

de Boyer Montégut C, Madec G, Fischer AS, Lazar A, Iudicone D (2004) Mixed layer depth over the global ocean: an examination of profile data and a profile-based climatology. J Geophy Res 09(C12)

Deser C, Alexander MA, Timlin MS (2003) Understanding the persistence of sea surface temperature anomalies in midlatitudes. J Clim 16:57–72

Dommenget D, Latif M (2002) A cautionary note on the interpretation of EOFs. J Clim 15:216–225

Dong S, Gille ST, Sprintall J (2007) An assessment of the Southern Ocean mixed layer heat budget. J Clim 20:4425–4442

Dwivedi S, Mishra AK, Srivastace A (2019) Upper ocean high resolution regional modeling of the Arabian Sea and Bay of Bengal. Acta Oceanol Sin 38:32–50

Fasham MJR (1995) Variations in the seasonal cycle of biological production in subarctic oceans: a model sensitivity analysis. Deep Sea Res 42:1111–1149

Fischer AS (2000) The upper ocean response to the monsoon in the Arabian Sea. PhD thesis, Mass. Inst. Of Technol/Woods Hole Oceanogr Inst

Fransner F, Counillon F, Bethke I, Tjiputra J, Samuelsen A, Nummelin A, Olsen A (2020) Ocean biogeochemical predictions-initialization and limits of predictability. Front Mar Sci 16(7):386

Frölicher TL, Sarmiento JL, Paynter DJ, Dunne JP, Krasting JP, Winton M (2015) Dominance of the Southern Ocean in anthropogenic carbon and heat uptake in CMIP5 models. J Clim 28:862–886

Gruber N, Gloor M, Mikaloff Fletcher SE, Doney SC, Dutkiewicz S, Follows MJ, Gerber M, Jacobson AR, Joos F, Lindsay K, Menemenlis D (2009) Oceanic sources, sinks, and transport of atmospheric CO2. Global Biogeochem Cycle 23(1)

Hanawa K, Talley LD (2001) Mode waters. In: Siedler G, Church JA, Gould J (eds) Ocean circulation and climate. Academic Press, San Diego, pp 373–386

Hunke EC, Dukowicz JK (1997) An elastic-viscous-plastic model for sea ice dynamics. J Phys Ocean 27:1849–1867

Jackett DR, Mcdougall TJ (1995) Minimal adjustment of hydrographic profiles to achieve static stability. J Atmos Ocean Tech 12(2):381–389

Johnson DR, Boyer TP, Garcia HE, Locarnini RA, Baranova OK, Zweng MM (2013) World Ocean Database 2013 user's manual

Kalnay E, Kanamitsu M, Kistler R, Collins W, Deaven D, Gandin L, Iredell M, Saha S, White G, Woollen J, Zhu Y (1996) The NCEP/NCAR 40-year reanalysis project. Bull Am Meteorol Soc 77:437–472

Kara AB, Wallcraft AJ, Hurlburt HE (2003) Climatological SST and MLD predictions from a global layered ocean model with an embedded mixed layer. J Atmos Ocean Tech 20:1616–1632

Khatiwala S, Primeau F, Hall T (2009) Reconstruction of the history of anthropogenic CO_2 concentrations in the ocean. Nature 462:346–349

Kidston J, Taschetto AS, Thompson DWJ, England MH (2011) The influence of Southern Hemisphere sea-ice extent on the latitude of the mid-latitude jet stream. Geophys Res Lett 38(15)

Large WG, Pond S (1982) Sensible and latent heat flux measurements over the ocean. J Phys Ocean 12:464–482

Large WG, McWilliams JC, Doney SC (1994) Oceanic vertical mixing: a review and a model with a nonlocal boundary layer parameterization. Rev Geophys 32:363–403

Levitus S (1982) Climatological atlas of the world ocean (vol 13). US Department of Commerce, National Oceanic and Atmospheric Administration

Lorbacher K, Dommenget D, Niiler PP, Köhl A (2006) Ocean mixed layer depth: a subsurface proxy of ocean-atmosphere variability. J Geophys Res Oceans 111(C7)

Lukas R, Lindstrom E (1991) The mixed layer of western equatorial Pacific Ocean. J Geophys Res 96:3343–3357

Lumpkin R, Speer K (2007) Global ocean meridional overturning. J Phys Ocean 37:2550–2562

Marshall J, Speer K (2012) Closure of the meridional overturning circulation through Southern Ocean upwelling. Nat Geosci 5:171–180

Marshall J, Adcroft A, Hill C, Perelman L, Heisey C (1997) A finite volume, incompressible Navier Stokes model for studies of the ocean on parallel computers. J Geophys Res 102:5753–5766

Martinson DG, Iannuzzi RA (2003) Spatial/temporal patterns in Weddell gyre characteristics and their relationship to global climate. J Geophys Res 108:8083

McCreary JP Jr, Kohler KE, Hood RR, Smith S, Kindle J, Fischer AS, Weller RA (2001) Influences of diurnal and intraseasonal forcing on mixed-layer and biological variability in the central Arabian Sea. J Geophys Res 106:7139–7155

Menemenlis D, Campin JM, Heimbach P, Hill C, Lee T, Nguyen A, Schodlok M, Zhang H (2008) ECCO2: High resolution global ocean and sea ice data synthesis. Mercat Ocean Q Newslett 31(October):13–21

Mitchell BG, Holm-Hansen O (1991) Observations of modeling of the Antartic phytoplankton crop in relation to mixing depth. Deep Sea Res 38:981–1007

Pellichero V, Sallée JB, Schmidtko S, Roquet F, Charrassin JB (2017) The ocean mixed layer under Southern Ocean sea-ice: seasonal cycle and forcing. J Geophys Res 122:1608–1633

Petty AA, Holland PR, Feltham DL (2014) Sea ice and the ocean mixed layer over the Antarctic shelf seas. Cryosphere 82:761–783

Pookkandy B, Dommenget D, Klingaman N, Wales S, Chung C, Frauen C, Wolff H (2016) The role of local atmospheric forcing on the modulation of the ocean mixed layer depth in reanalyses and a coupled single column ocean model. Clim Dyn 47:2991–3010

Sabine CL, Feely RA, Gruber N, Key RM, Lee KH, Bullister JL, Wanninkhof R, Wong CS, Wallace DWR, Tilbrook B, Millero FJ, Peng TH, Kozyr A, Ono T, Rios AF (2004) The oceanic sink for anthropogenic CO_2. Science 305:367–371

Sallée JB, Matear RJ, Rintoul SR, Lenton A (2012) Localized subduction of anthropogenic carbon dioxide in the Southern Hemisphere oceans. Nat Geosci 5:579–584

Sloyan BM, Rintoul SR (2001) The Southern Ocean limb of the global deep overturning circulation. J Phys Ocean 31:143–173

Smith W, Sandwell D (1997) Global sea floor topography from satellite altimetry and ship depth soundings. Science 277:1956–1962

Somavilla R, González-Pola C, Fernández-Diaz J (2017) The warmer the ocean surface, the shallower the mixed layer. How much of this is true? J Geophys Res 122:7698–7716

Sutton PJ, Worcester PF, Masters G, Cornuelle BD, Lynch JF (1993) Ocean mixed layers and acoustic pulse propagation in the Greenland Sea. J Acoust Soc Am 94:1517–1526

Talley LD (2013) Closure of the global overturning circulation through the Indian, Pacific, and Southern Oceans: schematics and transports. Oceano 26:80–97

Verdy A, Dutkiewicz S, Follows MJ, Marshall J, Czaja A (2007) Carbon dioxide and oxygen fluxes in the Southern Ocean: mechanisms of interannual variability. Global Biogeochem Cycles 21(2)

Villas Bôas AB, Ardhuin F, Ayet A, Bourassa MA, Brandt P, Chapron B, Cornuelle BD, Farrar JT, Fewings MR, Fox-Kemper B, Gille ST (2019) Integrated observations of global surface winds, currents, and waves: requirements and challenges for the next decade. Front Mar Sci 24(6):425

Winton M (2000) A reformulated three-layer sea ice model. J Atmos Ocean Techn 17:525–531

Wyrtki K (1964) The thermal structure of the eastern Pacific Ocean. Dstch Hydrogr Zeit Suppl Ser A 8:6–84

Yesubabu V, Kattamanchi VK, Vissa NK, Dasari HP, Sarangam VB (2020) Impact of ocean mixed-layer depth initialization on the simulation of tropical cyclones over the Bay of Bengal using the WRF-ARW model. Meteorol Appl 27:1862

Yuan XI (2004) ENSO-related impacts on Antarctic sea ice: a synthesis of phenomenon and mechanisms. Antarct Sci 16:415–425

Yuan X, Martinson DG (2000) Antarctic sea ice extent variability and its global connectivity. J Clim 13:1697–1717

Zhang KQ, Marotzke J (1999) The importance of open-boundary estimation for an Indian Ocean GCM-data synthesis. J Mar Res 57:305–334

Zhang J, Rothrock DA (2003) Modeling global sea ice with a thickness and enthalpy distribution model in generalized curvilinear coordinates. Mon Weather Rev 131:845–861